A SPECTROGRAPHIC ANALYSIS OF NOVA VULPECULAE 1968, NO. 1

J. B. HUTCHINGS
Dominion Astrophysical Observatory

Received January 5, 1970

The results of radial velocity measurements, line identifications, and line profile reductions on medium dispersion spectra of the nova are summarized. The velocity relations and line profiles are discussed together with published light curves of the nova. It is deduced that two main shells were ejected and accelerated away from the photosphere, and geometric and physical parameters are derived for the first 100 days after outburst. The nature of the acceleration is discussed and contrasted with the slow Nova Delphini 1967.

I. Introduction

Nova Vulpeculae 1968 No. 1, discovered by Alcock and Midtskoven (Marsden 1968) was a fast nova which had a peak visual magnitude of about 4.5 on April 17, 1968. Twenty-four spectrographic observations at dispersions of 15 and 60 Å/mm were made of the nova between April 17 and July 22, by which date the nova was about magnitude 9.5 and had a well-developed nebular spectrum. The spectrograms were all on IIa-O emulsion, covering the spectral range λλ 3300 to 5000, and were taken on the Cassegrain spectrograph of the Victoria 72-inch telescope. The journal of observations is given in Table I.

Radial velocity measurements of the strongest emission and absorption lines were made on all plates, and a detailed analysis of all lines was made from microphotometer tracings of the seven plates marked with an asterisk in Table I. The results are given in section II and an interpretative discussion is given in section III.

II. Results

The Radial Velocities. The velocities of absorption components of as many as possible of the Balmer lines Hβ to H9 and Ca II H and K were measured on all plates, and these velocities, corrected to the sun, are shown in Figure 1 and Table II. In general there were two main absorption components, and the two columns separate the high- and low-velocity groups, whose standard errors of measurement are about 50 and 25 km/sec respectively. Figures in parentheses are less accurate, and several other velocities of lower weight

TABLE I

THE DISTRIBUTION OF SPECTROGRAPHIC OBSERVATIONS

Date 1968	JD	Approx. m_v	No. of Spectrograms	Dispersion (Å/mm)
April 17	2439964.02	4.4	6	60
21*	68.01	5.2	1	15
22	69.00	5.3	1	15
24	70.91	5.4	1	15
May 1	77.90	5.8	1	15
2*	78.90	5.8	2	15
11	87.98	6.7	1	15
13*	89.92	6.8	1	15
16	92.93	7.0	1	15
17	93.91	7.1	1	15
18	94.88	7.1	1	15
23*	99.95	7.3	1	15
29	05.93	7.6	1	15
31*	07.90	7.8	1	15
June 20*	27.94	8.3	1	60
July 1	38.88	8.7	1	60
21	58.88	9.2	1	15
22*	59.84	9.2	1	15

*Microphotometer analysis made of these plates.

are not included. Each group showed increasing displacement with time and often were split into two or more sharper components. From a study of microphotometer tracings it was possible to study the variation of velocity of most of these components from plate to plate, and the lines drawn in Figure 1 show their accelerations. The mean velocities from the microphotometer tracings are also shown in Figure 1.

The emission components were generally very broad and amorphous so that it was difficult to derive meaningful or accurate velocities for them until the spectrum reached the nebular stage and the continuum was very weak. These profiles and velocities are described in more detail below, where a brief summary of the spectrum is given for each of the seven plates analyzed.

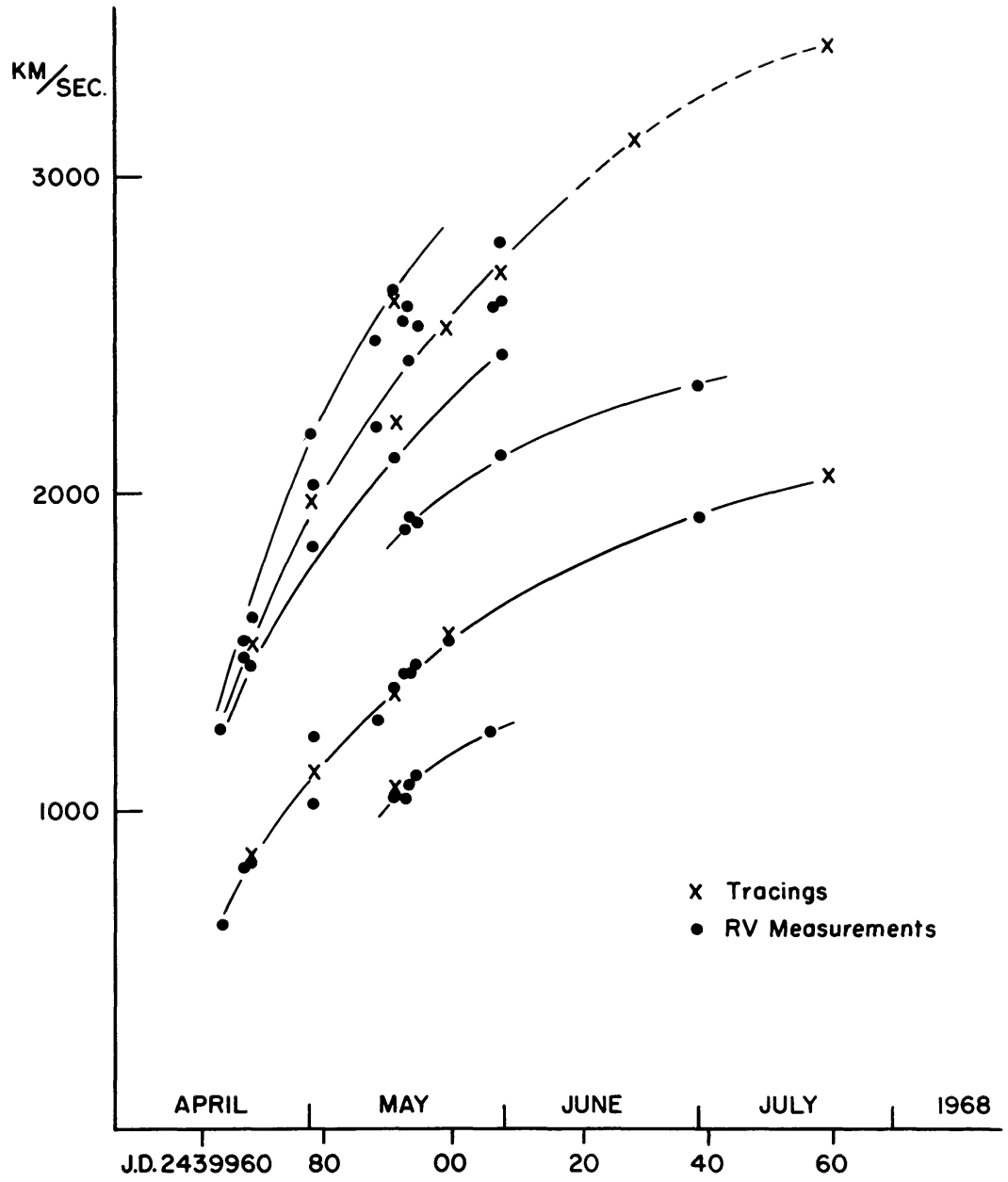

FIG. 1 — The mean heliocentric absorption line velocities from all plates and tracings, with the suggested velocity relations. All velocities are negative.

April 21. The spectrum has many lines, most of which have emission components which have developed since the light maximum on April 17. The breadth of the emission lines (some 1000 km/sec wide) and their erosion by adjacent absorption lines made

TABLE II

The Mean Line Velocities From Measurements of the Strong Balmer and Ca II Lines

Date 1968	Velocities* (km/sec)				
April 17	−635 (5)	−1260 (4)			
21	−810 (5)	−1480 (4), −1530 (2)			
22	−825 (4)	−1450 (4), −1600 (3)			
24	−940 (1)				
May 1	(−900)(1)				
2	−1020 (4), −1220 (2)	−1820 (4), −2020 (3)			
11	−1280 (5)	−2200 (3), −2480 (4)			
13	−1030 (4), −1380 (5)	−2110 (2), −2620 (5)			
16	−1030 (7), −1420 (5)	−1880 (3), −2540 (5)			
17	−1070 (7), −1420 (5)	−1920 (2), −2420 (3), −2580 (3)			
18	−1100 (5), −1460 (3)	−1900 (3), −2520 (4)			
23	−1530 (4)	−2520 (5)			
29	−1240 (2)	−2570 (3)			
31		−2110 (1), −2440 (2), −2600 (3), −2780 (1)			
June 20	(±800 em) (7), (±1500 em) (2)				(−3100) (1)
July 1	−830 (1), em as above, −1920 (1), −2330 (1)				
21-22	±850 em (4), ±1600 em (4)				(−3400) (1)

*The number of lines measured in each case is given in parentheses, here and also in Tables III and IV.

their measurement impractical. Table III gives the mean velocities of absorption components of lines of different ions for this plate, and the number of lines used is given in parentheses. Usually fewer lines were used than the total number identified because low-weight velocities (arising from blends or low plate density) were not included in the mean. The lines included under 'others' are lines of C I, Sr II, Sc II, Mg II, and Fe I.

TABLE III

APRIL 21 MEAN ABSORPTION LINE VELOCITIES

Ion	Identified Lines	Low Velocity (km/sec)	High Velocity (km/sec)	Mean Lower Excitation Potential (volts)
H	11	−876 ± 5 (7)	−1522 ± 8 (8)	10.2
Fe II	15	−858 ± 3 (14)	−1520 ± 5 (10)	2.8
Ti II	19	−843 ± 5 (15)	−1525 ± 7 (6)	<2.6
Cr II	6	−840 ± 3 (4)	−1509 ± 30 (3)	~4
Ca II	2	−886 3 (1)	−1453 (1)	
Others	17	−848 ± 3 (8)	−1510 ± 2 (2)	

The differences between the low-velocity figures for H, Fe II, and Ti II + Cr II are possibly significant. However, there is no definite correlation with excitation potential and the differences are not repeated in the high velocities, so that the phenomenon is not clear cut. The spectrum here is at its richest in lines (the April 17 plates have insufficient resolution to reveal any more), and the excitation temperature indicated by the lines present is about 7500° K. A very approximate spectral type for this spectrum is an A9 or F0 supergiant, which is in reasonable agreement with the temperature deduced.

May 2. The spectrum shows fewer and broader lines, and the emission-line peaks have increased in strength. The lower-velocity absorption has some signs of structure but not sufficient to warrant detailed measurement. Table IV shows the mean velocities of absorption. The term 'others' includes an additional La II line, while C I and Sc II were not detected. Only two Cr II lines were identified.

The scatter of these velocities is higher than for the previous plate, and there are no significant differences between ions. The spectrum is about the same as that of April 21.

TABLE IV

MAY 2 MEAN ABSORPTION LINE VELOCITIES

Ion	Identified Lines	Low Velocity (km/sec)	High Velocity (km/sec)
H	12	−1099 ± 20 (8)	−1961 ± 14 (9)
Fe II	9	−1112 ± 30 (7)	−1970 ± 21 (6)
Ti II	7	−1166 (2)	−2011 (3)
Ca II	2	−1152 (1)	−1977 (1)
Others	6	−1121 (3)	−2010 (4)

With the passage of time the absorption lines shifted further to the violet, became broader, and were accompanied by broader emission components. Thus it became increasingly difficult to measure and identify lines. This is particularly true of the region λλ 4580 to 4680 which contains many strong lines of Fe II, Cr II, and Ti II in the early postmaximum spectrum, O II and N II in the Orion stage (if any), and nebular lines in the final emission spectrum.

May 13. On this plate there are clearly four main absorption components in the hydrogen spectrum and at least two in the Fe II lines, as shown in Table V. All other lines were only tentatively identified and ten lines were unidentified or badly blended.

TABLE V

MAY 13 MEAN ABSORPTION LINE VELOCITIES

Ion	Identified Lines	Velocities in km/sec
H	9	−1057 ± 6 (6), −1373 ± 2 (6), −2221 ± 12 (4), −2620 ± 20 (6)
Fe II	7	−1354 ± 15 (4), −2213 (1)
Ti II	4?	
Cr II	2?	
Ca II	2	−1363 (1) −2630 (1)

Other lines possibly present are Y II, N II, and N III. A curious feature which appears at this time and remains until the continuum fades completely is a broad, strong and smooth absorption at about λ 4050. From the strength and position of the feature it is unlikely to be the O II λ 4070 blend. It is possibly connected with the Si IV

and N III lines near Hδ. If it is Si IV λ 4088, its displacement on this plate corresponds to a velocity of −3000 km/sec.

May 23. On this plate there is more definite evidence for the emergence of at least two high-temperature lines (N II and C II) and possibly of nebular [O III]. There is some structure in the strong Balmer emission lines suggesting four peaks at velocities +360, +100, −90, −360 km/sec. There are at least two absorption components to the Balmer lines, the stronger of which is at some −2500 km/sec, and the other at −1540 km/sec. The numbers of lines identified are H, 10; Fe II, 5; Ti II, 3; Cr II, 1; Ca II, 2.

May 31. The emission lines have not developed further structure and in the case of the Balmer lines, have a main positive velocity peak whose displacement decreases along the series from +300 km/sec at Hβ to +150 km/sec at H12. Three more N II lines may be present and no Ti II was definitely identified. The only reliable absorption velocity is about −2700 km/sec in the Balmer lines, although there are weak components around −2100 and −1700 km/sec.

During the second half of May a broad absorption was present near λ 4280 which moved to the violet with time. It may be the O II λλ 4317-19 blend with a velocity of some −2800 km/sec, but this is uncertain because of the presence of blended Fe II, Sc II, and Ti II lines.

June 20. This is a lower dispersion (60 Å/mm) plate so that a number of features may be poorly resolved. The spectrum is clearly nebular, with no sign of Fe II left. The only strong absorption feature is that at λ 4050. The nebular [O III] lines are present, as are the emission lines of He II λ 4686, N III, N II and O II blend at λλ 4634-41, and probably N V at λλ 4609 and 4625. All the emission profiles are strong with very steep sides. The edges of the six measurable Balmer lines lie at +830 km/sec and −700 km/sec.

July 22. The spectrum shows very strong emission lines of hydrogen, [O III], [Ne III], He II, He I, and N III. All have a strong central core (possibly with weak structure at the top) and wings extending to a fairly well-defined limit. The mean profile has limits at +1560 and −1600 km/sec and a core extending from +860 to −800 km/sec. The standard deviation of the means of the 14 lines is about ±60 km/sec. The best-defined edge is the redward edge of the

core, with a standard deviation of ±30 km/sec. Absorption components of Hγ are detectable in the weak continuum with a minimum at −2050 km/sec and a violet extent of about −3500 km/sec.

Interstellar Lines. The Ca II H and K lines had sharp interstellar absorptions which were detectable on most plates. The mean velocity from all measurements on all plates is −15.5 ± 0.9 km/sec. It is not possible to see whether the absorption consists of more than one component.

The Line Profiles. Figure 2 shows a series of rectified normalized tracings of the Hγ region throughout the spectral evolution of the nova. The first plate was taken within hours of maximum light and very weak emission is present. The growth of the emission strength during the following days is evident up to May 2, after which the peak intensity is apparently steady until the nebular spectrum develops in June.

The dotted lines in Figure 2 are the suggested true Hγ emission profiles, taking into account other blended lines. The absorption components are seen to be strong and broad until the end of May, with the exception of the additional multiple sharp absorption components shown in the May 17–18 profile. These sharp lines appeared about May 13 and disappeared by May 23, when the emission lines showed some brief four-component structure. After about May 20 the emission began to grow narrower, and the strong nebular lines had a sharp cutoff at about ±900 km/sec. [O III] λ 4363 can be seen from the end of May. Hγ emission increased in intensity up to July 1, after which it fell slowly, while the [O III] line increased in intensity more rapidly after June 20 and continued to rise at least until July 22. The intense central region in the July profiles is the result of the overlap of the two lines. The intensities at the top of these nebular profiles are not very reliable, but there is no strong evidence of line structure at this stage.

III. Discussion

The Line Profiles. From about one week after maximum light (when the emission components attained full strength) to the beginning of the nebular stage the line profiles retained the same basic shape. The emission peak of Hγ stayed at about twice the continuum intensity and the widths of the absorption components were proportional to their displacements. It has previously been shown

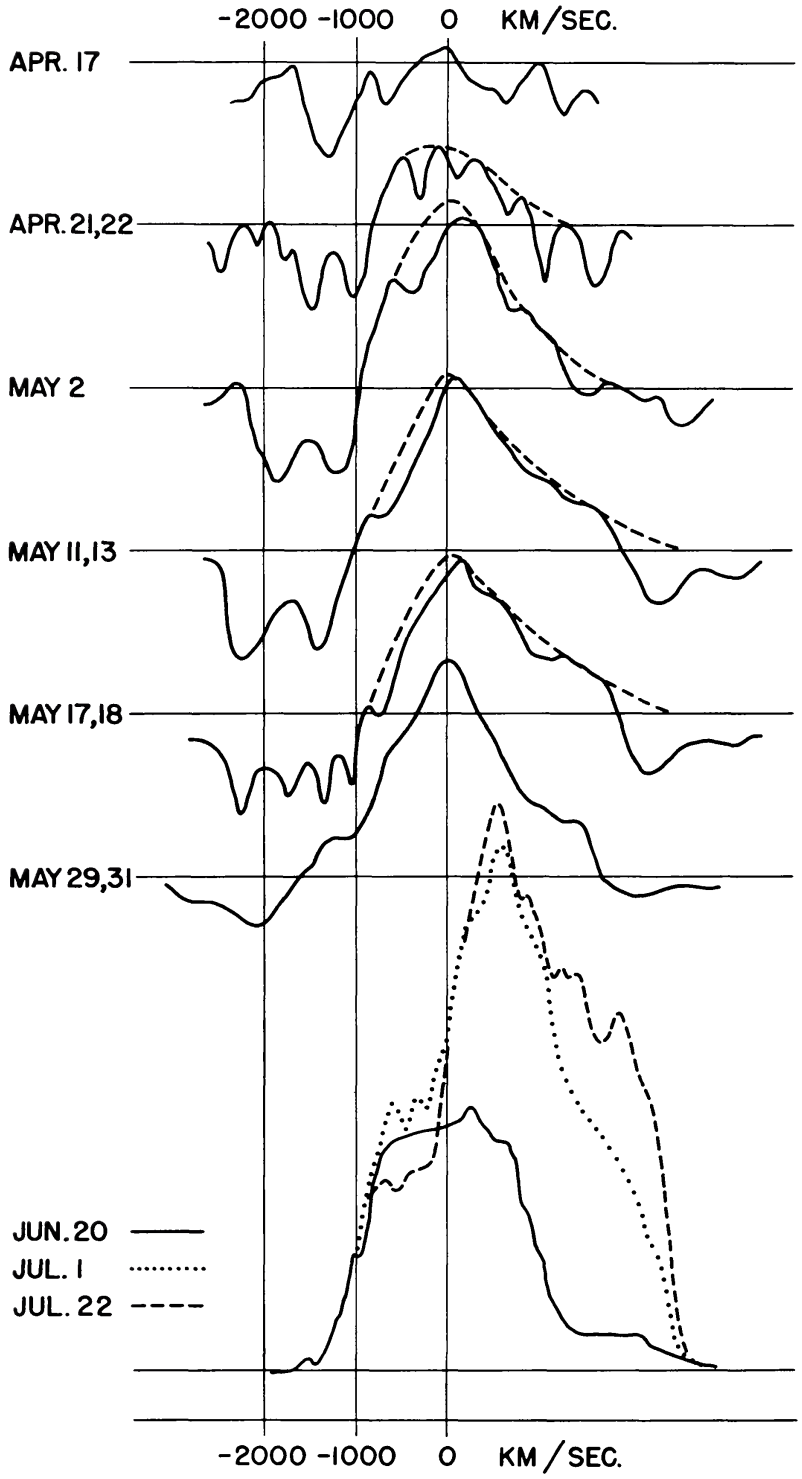

FIG. 2 — Mean rectified normalized tracings of the Hγ region throughout the spectral evolution. The continuum intensity in all except the last three tracings is the spacing between horizontal axes.

(Hutchings 1970*a*) in considerations of nova ejecta that there are two basic types of profile corresponding to the extremes of (*a*) a continuous extended envelope attached or close to the photosphere and (*b*) a thin shell moving away from a stationary or slower moving photosphere. The profiles in this nova lie somewhere between the two, but they are closer to type *a* in that the emission intensity does not fall in time and the absorption components do not become narrower and weaker. In the case of the slow Nova Delphini 1967 the existence of type-*a* profiles during the light-curve rise was taken to indicate a photosphere expanding at a rate comparable to that of its envelope. In the case of Nova Vulpeculae the distances implied and the rapid fall of luminosity indicate that the same situation cannot exist here. As it is clear that the profiles are not of either type, the hypothesis is proposed, which will be supported by further arguments, that the nova envelope consists of two or more geometrically thick shells which are accelerating away from the photosphere so that a velocity gradient within the shell along the cylinder of absorption causes the observed width and strength of absorption. This is analogous to the situation in extended envelopes of OB stars which are losing mass.

The Velocity and Light Curves. Figure 1 shows that the velocity curves are very smooth. The lines drawn represent the acceleration of the strongest absorption components, and they are slightly reinforced by some measurements of lower weight not included in the diagram. The increase in velocity seen in all components recalls the fact that type-*b* profiles (from an expanding thin shell) show an apparent increase in velocity as the corridor of absorption becomes narrower with increasing distance from the photosphere (Hutchings 1970*a*). Calculated profiles show, however, that this apparent increase in velocity is only some 25 percent for a realistic model of a nonaccelerating shell and in any case can never be greater than 100 percent. Further, almost all the apparent acceleration takes place below about five photospheric radii. As we show below that the acceleration in Nova Vulpeculae continues at heights much greater than this, we are justified in believing the observed acceleration to be a true one.

Photmetric observations of the nova have been published by Abuladze (1969), Grygar and Kohoutek (1969), and Fernie (1969). The visual light curves obtained by these workers are shown in

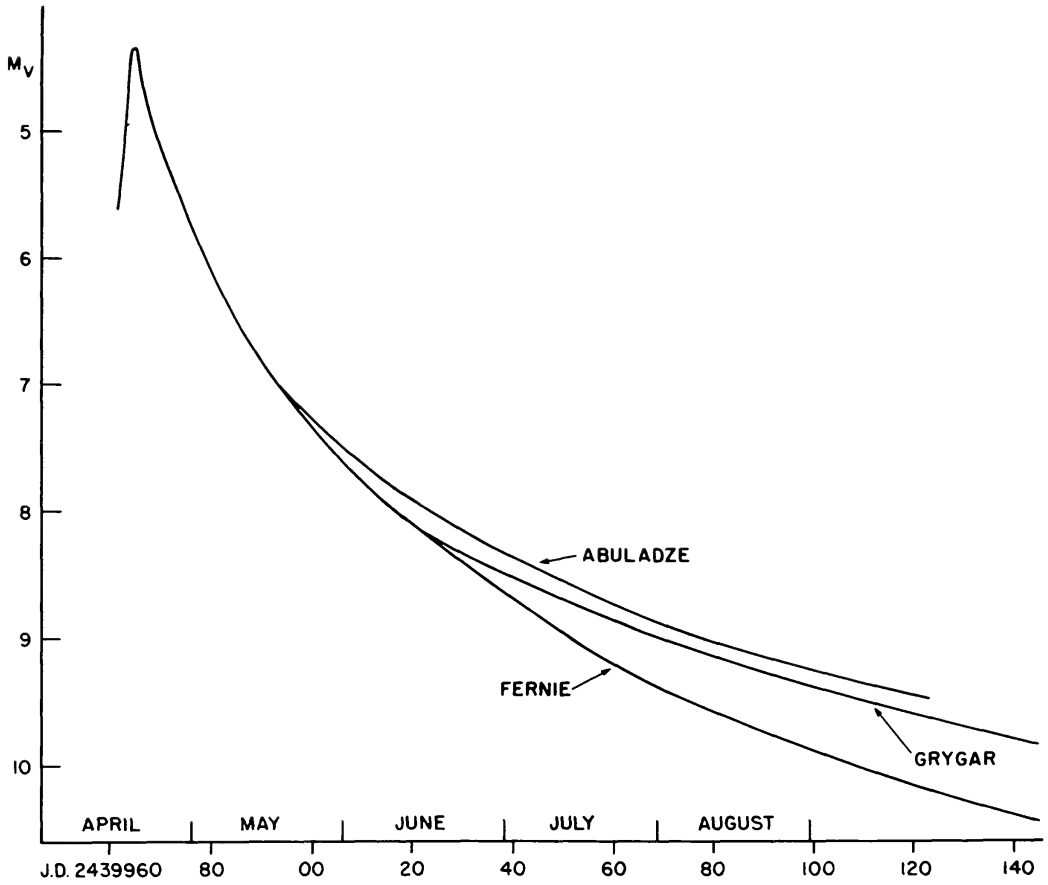

FIG. 3 — Published *V* magnitudes for Nova Vulpeculae by various workers.

Figure 3. The discrepancies in these results after about mid-June must be due to the inclusion of some strong emission lines in the *V* passbands of Grygar and Abuladze. This conclusion is confirmed by the fact that the curve of Abuladze begins to level off at the time at which [O III] is first detected in the spectrum and that of Grygar at the time at which the nebular lines grow rapidly in strength. Further evidence for this is in the *B* observations (which include most of the strong emission lines) of Fernie, which begin to fall less rapidly than the *U* and *V* at the same time. We therefore assume that the *V* observations of Fernie represent the continuum of the star most closely. The *U* observations include the Balmer recombination spectrum, whose strength must also depend on the nebular conditions. It is remarkable that the luminosity relation is very smooth. The smoothness of the velocity and light curves, the sym-

metry of the emission profiles, and the absence of strong structure in the nebular lines all suggest that the nova is a well-behaved one—in which photosphere and ejecta retain symmetry to a reasonable extent throughout the phenomenon.

The Size of the Shells and Photosphere. The velocity-time curves drawn in Figure 1 may be integrated to form distance-time curves and hence velocity-distance curves whose shapes are similar to those in Figure 1 (with distance the abscissae). This integration requires extrapolation to zero velocity at about April 4, which agrees well with an extrapolation of the light curve back to the initial magnitude suggested by Fernie. The velocity-distance curves bear a strong resemblance to the curves representing the radiative acceleration of high-energy ions from the surface of OB supergiants (Hutchings 1970*b*). The conditions under which radiative acceleration occurs (Lucy and Solomon 1970) are high radiation intensity, low gravity and density, and strong line opacity. At the peak intensity of the nova $M_v \sim -8$ (Fernie 1969) and from Figure 1 the radius of the innermost shell is about 5×10^8 km, yielding probable values of $\log g < 1$ and $\rho < 10^{-12}$. There are many strong lines in the spectrum so that the conditions for radiative acceleration seem to be fulfilled. If we therefore follow the arguments of Hutchings (1970*b*) for the velocity-distance curves derived from Figure 1 we can show that the velocity reaches half its terminal value at a height of some three photospheric radii. This leads to a mean estimate for the photospheric radius of 3×10^8 km at April 26. We must assume that the photosphere expanded with the inner envelope until maximum light, to explain the light maximum and because no significant emission lines were present until after maximum light (see also Mammano, Margoni, and Rosino 1969). The photospheric radius at this time was thus some 5×10^8 km, so that the figures suggested above imply the shrinking photosphere we expect from the light curve.

We may further consider the photosphere in terms of a gravitational collapse. The mass lost by a nova outburst is a very small fraction of the total and we may assume that the star retains a high central concentration at all stages. The gravitational potential within the extended photosphere is to a first approximation simply related in the usual way to distance from the center. Even if only 70 percent of the mass remains in the central condensation the

conclusions below are practically unaffected. It is clear that the inner regions of the photosphere will collapse rapidly while the outer regions, which are on the verge of radiative acceleration, will not collapse at all in the time scale of the observations. If the original star had a mass of 2 $\mathfrak{M}_\odot$, the innermost 3×10^8 km will collapse completely in 100 days. The collapse rate of the photosphere and density-height relations were computed for a number of different initial extended photosphere structures. A rigorous treatment of this problem involves pressure and heating effects; these were neglected in this simple model, and the photosphere was assumed to be represented by the radius to a certain density. The observational constraints on the radius are that it must allow the rapid light fall-off from maximum without strong initial heating, and that the collapse rate should decrease with time as indicated by the light curve. This effectively restricted the model to one with an exponential density scale of 10^7 km, giving a reasonable photospheric density (10^{-6} gm/cm^3) initially near 3×10^8 km. Even this does not predict the rapid postmaximum shrinkage required by the light curve and suggested by the acceleration argument above. However, since the shells are accelerated strongly away from the 5×10^8 km radius photosphere it is very probable that the outer half of this photosphere itself dispersed outwards under radiation pressure rather than collapsing under the extremely weak gravitational force ($\log g \leqslant 0$). This would lead to the rapid shrinkage of the photosphere down to a level where gravitational collapse takes over. Thus we derive the suggested photospheric radius curve shown in Figure 4.

The Temperature and Light Curve. Using the relation of Figure 4 we can now derive the photospheric temperature as it collapses, assuming the *V* luminosity to be proportional to the surface area and the Planck function at 5500 Å. From the spectral analysis, we assume the effective temperature of the extended photosphere at maximum light to be a little below the 7500° K derived for April 21, and for convenience 7000° K was used, acknowledging the possibility of a zero-point error of some 300° K. We can now derive the temperature relation shown in Figure 5, using Fernie's *V* magnitudes. These temperatures seem quite compatible with the observed spectra (hydrogen maximum absorption at mid-May at 8200° K, close to the Saha-Boltzmann maximum for low pressures;

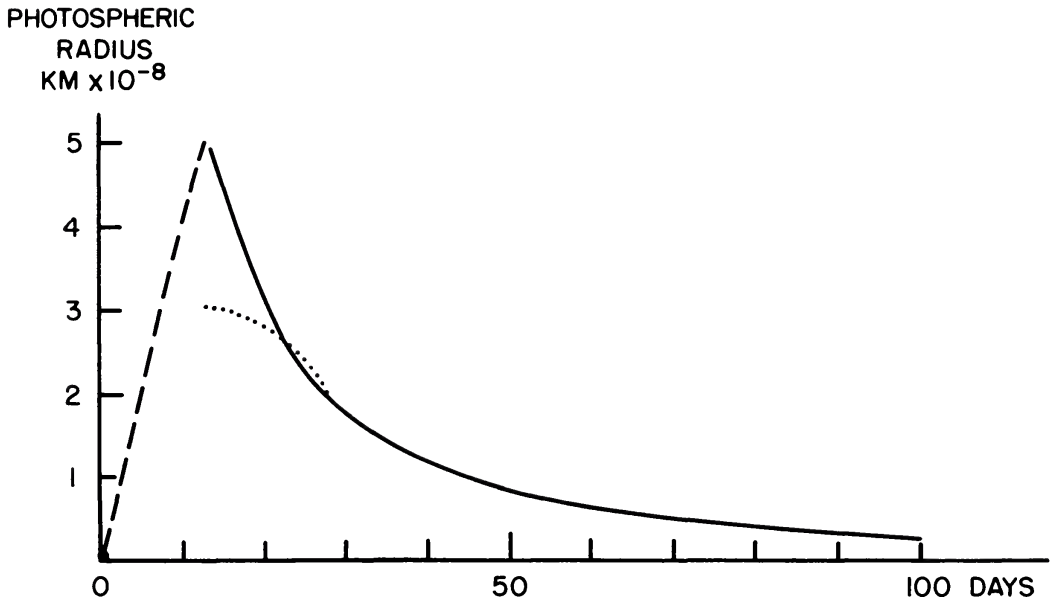

FIG. 4 — The deduced photospheric radius as a function of time from outburst. Dotted line represents pure gravitational collapse.

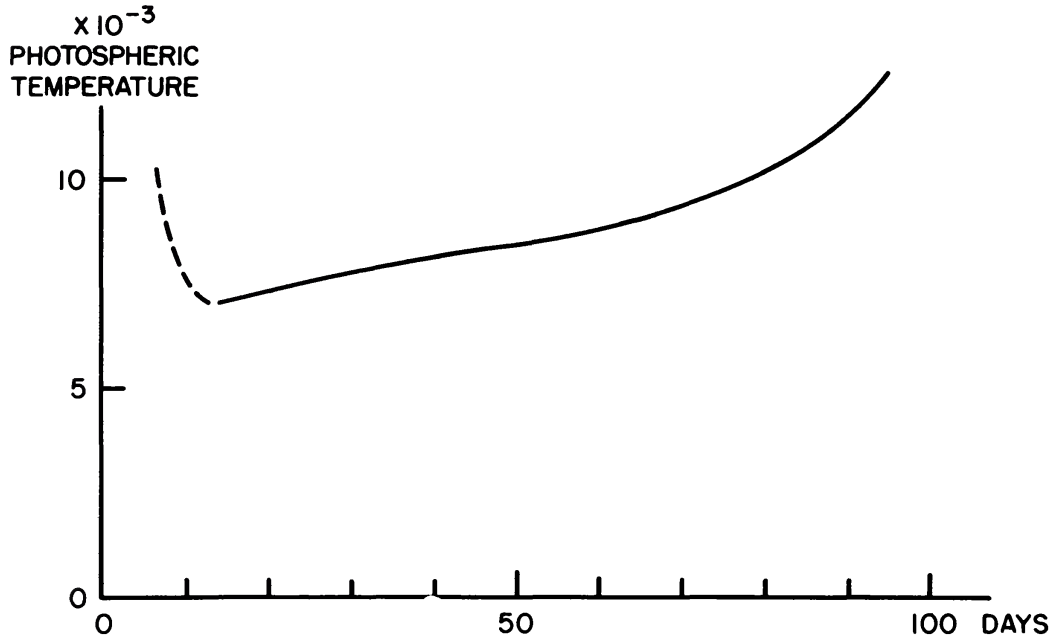

FIG. 5 — The deduced photospheric effective temperature after maximum light.

nebular lines of O III strong after mid-June at above 9500° K, the temperature required for O III photoionization).

Looking back at the profiles in Figure 2 we can check these results further against spectral behavior. The Hγ emission profile is at its broadest at about May 15, when the photosphere is about 0.2 of its maximum radius. The dilution W for the two main shells is 0.003 and 0.001 and the temperature is 8200° K. The multiple sharp absorption components visible for a few days could be caused by short-lived nonuniformities in the shrinking photosphere, either in the form of holes revealing the hot interior or of condensations of high opacity. The fact that the structure was present in all strong lines suggests that the cause is a geometrical one. The short-lived emission-line structure observed on May 23 may also be connected with this fragmentation. The weakening high-velocity emission and absorption observed after this date represents the evolution of a type-*b* profile and is therefore compatible with the relatively small size and temperature deduced for the photosphere. Evidently most of the nebular spectrum arises in the slower-moving inner layers of the ejected matter, where oxygen is most readily ionized by the central star.

Finally it is instructive to contrast this nova with the exceptionally slow Nova Delphini 1967. In the latter no acceleration of ejecta occurred either during or after the initial rise and it is important to understand the difference in physical conditions causing these different forms of behavior. At present only a few suggestions can be made. From the prenova identifications and distance moduli for the two novae it is apparent that Nova Vulpeculae reached a peak luminosity some 30 times (2^m5) that of Nova Delphini (see Hutchings 1970*a*), and was brighter than Nova Delphini for the first 50 days after initial outburst. Nova Vulpeculae did not reach the same photospheric extension as Nova Delphini so that its radiation pressure was considerably higher throughout the initial stages. However, radiation pressure cannot be the only cause of the acceleration as Nova Vulpeculae continued to accelerate after its luminosity fell below that of Nova Delphini. It is probable from the discussion above that Nova Delphini had a higher shell density, in which collisions were more frequent, and where more radiative momentum is required to produce an acceleration. The argument must naturally apply to novae in general, and it is worth noting that accelera-

ting velocities are found only in novae of higher luminosity, although not in all such novae.

We may make a crude estimate of the mass lost by the nova. The O III nebular lines first appear (about May 20) at a shell radius of about 50×10^8 km, when the density is probably some 10^7 particles/cm^3, as estimated from the velocity curves and density zero point. The total thickness of all shells at this radius is about 20×10^8 km, yielding a total mass lost of $3 \times 10^{-6}\ \mathfrak{M}_\odot$.

IV. Conclusion

From the radial velocity curves and derived line profiles it is proposed that the nova outburst consisted of the ejection of two main shells from an extended photosphere. Preserving approximate spherical symmetry, these shells accelerated away from the photosphere which collapsed and heated up after maximum light. The geometrical configuration of the shells and photosphere and the photospheric temperature were suggested for the hundred days following the outburst and shown to be consistent with the observed spectrum. The cause of the acceleration may be the conditions of radiation intensity and shell density at maximum light.

The above approach is obviously an extremely simplified one and must be tested on further novae. A deeper treatment of the theoretical implications is important in justifying the shell hypothesis and for comparison with shock-wave theories. As novae appear to be highly individual events it may be that different physical processes apply in different cases, and for this reason we have avoided the standard classificatory remarks on the spectrum and light curve.

I am indebted to a number of Dominion Astrophysical Observatory astronomers for obtaining most of the spectra, to W. A. Fisher for work on the line-profile reductions, and to J. Grygar for some discussions.

REFERENCES

Abuladze, O. P. 1969, *I.A.U. Comm. 27, Inf. Bull. Var. Stars*, No. 324.
Fernie, J. D. 1969, *Pub. A.S.P.* **81**, 374.
Grygar, J., and Kohoutek, L. 1969, *B.A.C.* **20**, 226.
Hutchings, J. B. 1970*a*, *Pub. Dominion Astr. Obs.* **13**, No. 16.
—— 1970*b*, *M.N.R.A.S.* **147**, 367.
Lucy, L. B., and Solomon, P. M. 1970, *Ap. J.* **159**, 879.
Mammano, A., Margoni, R., and Rosino, L. 1969, in *Non-Periodic Phenomena in Variable Stars*, L. Detre, ed. (Dordrecht: D. Reidel), p. 271.
Marsden, B. 1968, *I.A.U. Circulars*, Nos. 2066 and 2067.